Relationships between pressure, flow, lip motion, and upstream and downstream impedances for the trombone

Henri Boutin,[a] Neville Fletcher, John Smith, and Joe Wolfe

School of Physics, The University of New South Wales, Sydney, New South Wales 2052, Australia

This experimental study investigates ten subjects playing the trombone in the lower and mid-high range of the instrument, B♭2 to F4. Several techniques are combined to show the pressures and the impedance spectra upstream and downstream of the lips, the acoustic and total flows into the instrument, the component of the acoustic flow due to the sweeping motion of the lips, and high speed video images of the lip motion and aperture. The waveforms confirm that the inertance of the air in the channel between the lips is usually negligible. For lower notes, the flow caused by the sweeping motion of the lips contributes substantially to the total flow into the mouthpiece. The phase relations among the waveforms are qualitatively similar across the range studied, with no discontinuous behavior. The players normally played at frequencies about 1.1% above that of the impedance peak of the bore, but could play below as well as above this frequency and bend from above to below without discontinuity. The observed lip motion is consistent with two-degree-of-freedom models having varying effective lengths. These provide insight into why lips can auto-oscillate with an inertive or compliant load, or without a downstream resonator.

[AH]   Pages: 1195–1209

I. INTRODUCTION

When producing sound on the trombone and other lip-valve instruments, the player's vibrating lips interact with the flow of pressurized air from the lungs and with the acoustic waves in two ducts; one downstream (the bore of the instrument) and one upstream (the player's vocal tract). Both the process of auto-oscillation—the conversion of a nearly steady pressure in the lungs into sustained acoustic waves in the instrument—and the sound it produces are of interest to acousticians. Their relationship is also potentially interesting to teachers, students, and players of brass instruments.

Several techniques have been used to study the lip-duct(s) interaction in lip-valve instruments. The pressure in the mouthpiece and its relation to the upstream steady pressure have been investigated (Bouhuys, 1965; Elliott and Bowsher, 1982; Yoshikawa, 1995; Fletcher and Tarnopolsky, 1999). Stroboscopy (Martin, 1942; Copley and Strong, 1996; Yoshikawa and Muto, 2003) and high-speed video (Newton *et al.*, 2008; Bromage *et al.*, 2010) have been used to study the motion of the lips directly. The electrical impedance across the lips has been used to study it indirectly (Wolfe and Smith, 2008; Fréour and Scavone, 2011, 2013), although a variable delay between the variations in electrical impedance across the lips and the lip aperture (Boutin *et al.*, 2014; Hézard *et al.*, 2014) makes it difficult to draw firm conclusions. The ratio and phase difference of the pressures measured in the mouth and bore of the instrument, and hence the ratio of the upstream to downstream acoustical impedance, has been measured for the trombone (Fréour and Scavone, 2013). The impedance spectra of the bore of a range of lip-reed instruments have been measured (e.g., Backus, 1976; Elliott *et al.*, 1982; Caussé *et al.*, 1984). The spectrum of the upstream acoustical impedance has been related to the spectral envelope of the sound of the didjeridu (Tarnopolsky *et al.*, 2005) and compared with the playing frequency in the trumpet (Chen *et al.*, 2012).

Models of the lip-duct interaction make a range of approximations. Qualitative treatments are given by Helmholtz (1877) and Benade (1976). Linearization of aspects of the lip motion and considering only small signals permit analytical solution for the conditions allowing auto-oscillation for a cantilever valve (Elliott and Bowsher, 1982; Fletcher, 1993). Artificial lips have been used to allow access to measurements of auto-oscillation in a system with controllable physical parameters (e.g., Gilbert *et al.*, 1998; Cullen *et al.*, 2000). A simple numerical model reproduces some of the observed properties (Adachi and Sato, 1996). The lip motion has been compared (Adachi and Sato, 1996) with that of the vocal folds in phonation (Ishizaka and Flanagan, 1972), which is another incentive to understanding it.

The acoustic flow out of the tract and into the instrument is related to the lip aperture, the pressures on either side of the lips and the impedances up- and down-stream. Usually, the instrument plays at a frequency close to a resonance of the bore, but the fundamental playing frequency may lie above or below the resonance of the bore (e.g., Yoshikawa, 1995; Chen and Weinreich, 1996; Campbell, 1999; Eveno *et al.*, 2014) or of the vocal tract (Chen *et al.*, 2012), so the phase angle between pressure and flow may have either sign. The motions of the lips in the longitudinal and transverse directions each have different phases (Yoshikawa and Muto, 2003), as must the two components of the flow: the flow

a)Author to whom correspondence should be addressed. Electronic mail: boutin@lam.jussieu.fr

passing between the lips and the flow swept by the moving lips. The magnitudes and phases of all these variables are important to understanding the lip-pressure-flow interaction.

So far, the authors know of no study that combines several techniques to show, for the same player and instrument, the pressures on either side of the lips, the impedance spectra upstream and downstream, the acoustic flow and steady flow into the instrument, the component of the acoustic flow due to the sweeping motion of the lips, and high speed video images of the lip motion. Providing such measurements is the principal object of the present paper. We also discuss the results in terms of some of the fundamental physics involved.

High-speed video images were analyzed to determine the aperture between the lips and the two principal lip motions in two planes. This allowed an estimate of the sweeping flow—the flow due to lip motion alone. Transducers measured the pressure up- and down-stream from the lips. The vocal tract impedance was measured during playing and the bore impedance was measured immediately after playing. This allowed calculation of the steady and acoustic flows into the instrument. Such measurements were made on several notes over the lower and mid-high range of the trombone, as played by ten players with a range of experience in playing the instrument.

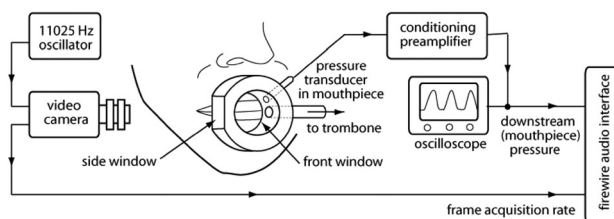## II. MATERIALS AND METHODS

A. Materials

1. The subjects

Ten trombonists spanning the range from beginner to professional volunteered as subjects in the experiment. Three had between 15 and 50 years of professional experience in band, orchestra, and jazz. Four were serious amateurs with extensive experience, between five and twelve years, in bands and orchestras. Three identified as beginners; one was an experienced trumpeter (six years of practice) with little experience on the trombone, one had orchestral trombone experience but had not played the instrument recently, and one was the first author who began learning the trombone for this project. The results of these beginners are not included in some of the analysis.
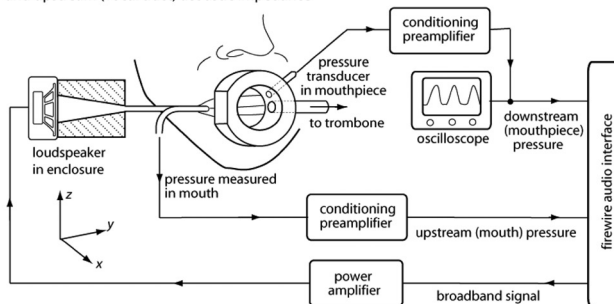
2. The instrument

The trombone is a Yamaha model YBL 321 with a B♭-F "trigger." The trigger valve that adds extra tubing was left in the shorter (B♭) position throughout the study. In the experiments, the subjects played while the main slide was first all the way in, and then extended by 22.7 cm. These positions, used to play the harmonic series starting on B♭2 (nominally 117 Hz), and three semi-tones lower on G2 (nominally 98 Hz), are, respectively, referred to as first and fourth positions by trombone players. (All pitches are given nominal frequencies using A440 tuning in equal temperament.) The tuning slide position was constant at 18 mm from the shortest, i.e., fully closed position. The instrument was mounted in a fixed position above a laboratory bench using padded clamps.
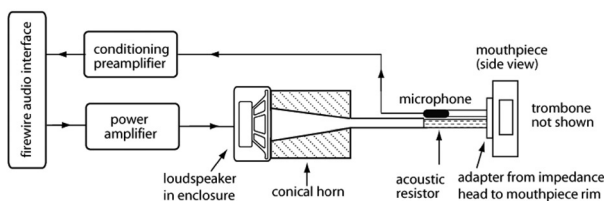

FIG. 1. Schematic diagram (not to scale) of the configurations of the experimental apparatus. For clarity the trombone and the mirror at 45° have not been shown.

3. The mouthpiece

The trombone mouthpiece was replaced by a transparent one having a shank of the same shape, a rim of the same diameter, and a cup with the same volume, as shown in Fig. 1(A). The cup shape was nearly cylindrical, with the shank set in one side, and two glass windows that allowed images of the lips from the front and the side, without distortion (Ayers and Lodin, 2000). A pressure transducer (8507C-2, Endevco, CA) was located inside the mouthpiece, near the rim, to measure the pressure downstream of the lip valve.

B. Methods and experimental protocols

1. Pressure variation within the mouthpiece cup

The extent of any variation in the acoustic pressure within the cup was determined by comparing the pressure signals measured at six different positions within the mouthpiece. This involved replacing the front window on the mouthpiece with a plate containing three sealable holes: one located on the axis x of the mouthpiece cup, see Fig. 1(B), and the others located 10 mm above and below the axis. During these measurements, the pressure sensor in the rim of the mouthpiece was left in place while a second similar transducer was inserted into the mouthpiece through one of

these three holes, the other two being sealed. For each hole, the tip of the transducer was located either flush with the inner face of the plate, or 15 mm inside the mouthpiece, this distance being the closest that it could be placed without touching the vibrating lips.

For each of the six possible positions of the second transducer, one of the subjects was asked to play with the slide in first position. The ratio of the signal from the re-locatable transducer to that of the transducer fixed in the rim was examined in the frequency domain. This experiment was repeated for three different notes (B♭2, F3, and B♭3). For each note, the ratio of the magnitudes of the microphone signals at the fundamental frequency was 1.00 ± 0.03 and the difference in phase was always less than $2.8°$. Thus, for acoustic signals with wavelengths much larger than the dimensions of the mouthpiece, the pressure in the mouthpiece was uniform to a good approximation.

2. General experimental protocol

In the next three experiments, subjects were asked to play notes while the slide was all the way in (first position) and then extended by 22.7 cm (fourth position). In first position, they were asked to play the notes *mp* in the ascending harmonic series: B♭2 (nominally 117 Hz), F3, B♭3, D4, F4, etc. In fourth position, they were asked to play D3, G3, B3, D4, etc. No further instruction was given regarding the pitch.

An oscilloscope in the subject's view showed the pressure waveform measured in the mouthpiece. In the initial experiments, two horizontal cursor lines across the screen were adjusted to show the upper and lower limits of the waveform. In subsequent experiments, these were used as a reference and subjects were asked to play the note with an amplitude equal to (within 10%) that measured in the first series.

3. Measuring lip geometry and downstream pressure

We define the axis of the mouthpiece as the x direction, y is horizontal and at right angles to x, and z is vertical, as shown in Fig. 1(B). In the first experiment, a high-speed video camera (X-stream VISION^{TM} XS-4 with Nikon Nikkor 35 mm f1.4 lens) captured images directly from the side of the lips and from the front via a mirror parallel to z and at $-45°$ from x. An oscillator was used to set the image acquisition rate at 11 025 frames per second. The exposure time was 62μs and the maximum length of each movie was 1.49 s.

Once the pressure downstream of the lip valve, i.e., in the mouthpiece, had started recording, the player started playing each note and then, when satisfied with the signal amplitude, pushed a switch to start recording images. The camera generated a square pulse corresponding to the acquisition of each frame; this was digitally recorded along with the pressure transducer output. This allowed the synchronization of images with the mouthpiece acoustic pressure signal, see Fig. 1(A).

4. Measuring up- and down-stream pressure and upstream acoustic impedance

The impedance in the mouth Z_{mouth} was measured during playing with a technique used previously (Tarnopolsky *et al.*, 2006; Chen *et al.*, 2012) using the experimental setup depicted in Fig. 1(B). Two small cylindrical ducts were glued together side by side producing an impedance head with an oval cross section with dimensions 4.8 mm $\times$ 7.8 mm. This was passed between the lips at the corner of the mouth and players were asked to locate the end at the center of their mouth between their upper and lower teeth. Players reported no difficulty in doing this. The end should thus be located close behind the lips. One duct was used to inject the current source and the other led to a pressure transducer (8507C-2, Endevco, CA). The current source was the sum of sine waves between 50 and 1000 Hz with spacing 0.67 Hz and the impedance head was calibrated using an acoustically infinite duct with diameter 26 mm and length 194 m (Dickens *et al.*, 2007). During calibration, the amplitudes of all the frequency components of the injected acoustic current were adjusted to be equal in the measured pressure (Smith *et al.*, 1997) and their phases adjusted to improve the signal to noise ratio (Smith, 1995).

Performers played repeated notes over a duration of 51 s, pausing to breathe at will. During these notes, 34 impedance measurements, each comprising 2^{16} samples at a sampling rate of 44.1 kHz were made. Each measurement thus took 1.5 s, giving a Fourier limit to frequency resolution of 0.67 Hz.

During this experiment, the acoustic pressures in the mouthpiece and in the mouth were also recorded by the pressure transducers on each side of the lip valve. During each measurement, the player viewed the oscilloscope while playing, as described above in Sec. II B 2, so that the pressure level in the mouthpiece was kept very similar to that recorded in the first experiment.

5. Measuring the steady pressure in the mouth

In a separate experiment, a plastic tube connected to a pressure gauge was inserted between the lips of the players at the corner of the mouth. For each slide position, they were asked to play each note while using the oscilloscope screen to ensure the amplitude of the mouthpiece pressure was similar to that in the two previous experiments. The pressure difference measured between the continuous component in the mouth and the atmospheric pressure, is henceforth called dc pressure by analogy with direct current in electronics. In practice, the players were able to reproduce the dc pressure within 10%. For one player, the dc pressure was also measured simultaneously during both the experimental configurations shown in Figs. 1(A) and 1(B). The data shown in Fig. 5 are from this player.

6. Measuring the bore impedance

The bore impedance was measured in the plane of the rim of the mouthpiece with a method similar to that used for Z_{mouth}, see Sec. II B 4, and using the setup shown in

Fig. 1(C). The impedance head used an acoustic current whose source was the air gap between a truncated cone and a conical hole, the two separated by three $100\,\mu$m diameter wires at $120°$ separations (Smith *et al.*, 1997). Adjacent to the source in the plane was a microphone (4944A, Bruel & Kjær, Denmark), used with a pre-amplifier (Nexus 2690, Bruel & Kjær, Denmark), and a Firewire audio interface (MOTU 828, Cambridge, MA). The impedance head was calibrated using an acoustically infinite duct of length 142 m and diameter 7.8 mm. The signal used for calibration and measurement used a sum of sine waves between 50 and 1.8 kHz, with a spacing of 0.67 Hz.

Near an impedance peak, the magnitude and phase of the bore impedance at the playing frequency vary significantly with small changes in the difference between the playing frequency f_p, and the frequency of the closest impedance peak, f_{peak}. f_{peak} depends on the temperature and composition of the air in the bore. During the measurements of playing in this study, the durations of the notes played ranged from 5 to 15 s approximately, with long gaps in between. For this reason the impedance spectrum of the bore (Z_{bore}) was measured as soon as practical after the (cool, dry) instrument has been played for 10 s. For the trombone, the combined effect of variations in composition and temperature after playing for several seconds is modest: it appears that the flattening effect of increased CO_2 is compensated to a large extent by the sharpening effect of temperature and humidity (Boutin *et al.*, 2013).

The impedance measurements commenced as soon as possible after playing stopped. In practice it took less than 3 s to place the impedance head into the plane of the mouthpiece rim and start measuring. Each experiment comprised 32 consecutive measurements, each of 1.5 s duration. The frequency and magnitude of nine impedance peaks were calculated for each successive measurement. Linear regression was then used to estimate the values of frequency and magnitude for each impedance peak at a time 3 s before the beginning of the first cycle, i.e., just before playing stopped.

C. Analysis of data

1. The aperture between the lips

The area of the aperture between the lips was estimated using a method similar to that of Bromage *et al.* (2010), by counting the dark pixels on the frontal view captured by the high-speed camera.

2. The acoustic flow

The definition of the bore impedance Z_{bore} relates the acoustic pressure in the mouthpiece downstream of the lips (p_{bore}) to the acoustic component of the flow into the mouthpiece and bore (u_{bore}). Measurements at different positions within the mouthpiece (see Sec. II B 1) showed little spatial variation of the acoustic pressure within the mouthpiece. The total acoustic flow into the bore, u_{bore}, was calculated by dividing the spectrum of the pressure measured at the mouthpiece rim by the bore impedance spectrum Z_{bore}, over the frequency range where Z_{bore} was measured (50 Hz to 1.8 kHz).

The acoustic flow coming out of the mouth was similarly calculated by dividing the acoustic pressure measured in the mouth (p_{mouth}) by the measured vocal tract impedance (Z_{mouth}), over the frequency range from 50 Hz to 1 kHz. The sign was reversed so that the flow traveling from the lungs towards the lips is positive.

3. The sweeping flow

The acoustic flow caused by the outward motion of the lips *per se* is an important variable. The camera recorded a time sequence of (x, z) and (y, z) images, but not (x, y). The volume of the lips inside the mouthpiece was calculated in the following way. The contour of the portion of the lips within the mouthpiece in the (x, z) plane was identified by inspecting the side view on each frame. Its area, bordered by the mouthpiece rim, was calculated. To estimate the effective width of the lips, one player was asked to turn the mouthpiece about the x-axis so that the side window was parallel to the (x, y) plane below the player's lips. A picture of the lip contour was taken through this window. The effective width was given by the surface covered by this contour, divided by the maximum deflection of the lips in the x-direction. The area of the cross-section, multiplied by the effective width of the lips, gives the volume displaced by the lips. The sweeping flow u_{sw} is the time derivative of this volume, which oscillates in the mouthpiece cup. The derivative was calculated by taking the Fourier transform, multiplying by $j\omega$, truncating above 400 Hz to filter out high frequencies, and then taking the inverse transform.

4. The steady flow

The flow of air through the channel formed by the aperture between the lips is defined as U_{ch} and the flow through the mouthpiece into the bore, henceforth called U_{bore}, is equal to U_{ch} plus the alternating sweeping flow u_{sw}. During every cycle, and for all players on all notes, there is a time when the lip aperture is closed and the lips are stationary; then both U_{ch} and the sweeping flow must be zero. During this brief interval U_{bore} will be zero and consequently its steady component $\bar{u}_{\text{bore}}$ and its alternating acoustic component u_{bore} will then cancel: $U_{\text{bore}} = \bar{u}_{\text{bore}} + u_{\text{bore}} = 0$. Consequently, the magnitude of the measured alternating component $-u_{\text{bore}}$ at this instant gives a measure of the constant steady flow $\bar{u}_{\text{bore}}$ into the mouthpiece. This value can then be added to the alternating component u_{bore} measured at any time to give the total flow (acoustic + steady) U_{bore} into the mouthpiece and bore at that time.

5. The horizontal and vertical lip deflections

The video sequences revealed that, on the front edge of each lip, different points did not move in phase. Thus the deflection of the lips in the x and z directions depends on the particular point considered. In order to simplify the lip motion, each lip is first represented by a single point oscillating in the (x, z) plane. On each video frame, the cross section of each lip in the (x, z) plane is measured on the side views, and divided by the height of the lip at the border with the mouthpiece rim. The resulting values, subsequently called $\hat{x}_{\text{up}}$ and $\hat{x}_{\text{low}}$, are used to estimate the horizontal deflections
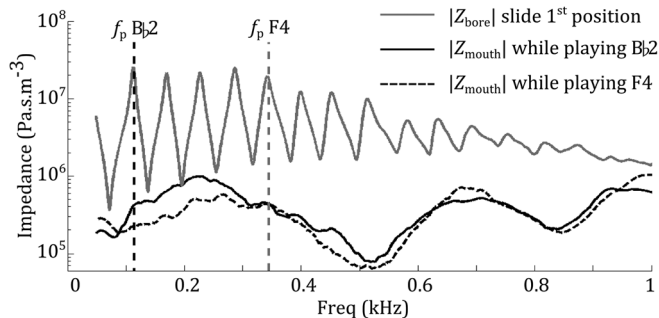
FIG. 2. The upper curve is the magnitude of the bore impedance while the slide is in first position. The lower curves are vocal tract impedances measured in the mouth while the player is playing B♭2 (solid) and F4 (dashed). The vertical dashed lines show the playing frequency f_p while playing B♭2 (black) and F4 (gray).

of the upper lip and the lower lip respectively. On the front view, the vertical separation between the lips is also measured, at a point where its amplitude is maximal. This magnitude, henceforth called z, is taken as a measure of the vertical displacements of the lips.

III. RESULTS

A. Impedance in the mouth while playing

During the first experiment, the impedance was measured in the mouth of each player while playing each note of the ascending harmonic series: B♭2 to F4 when the slide was in first position and D3 to a note near F4 when it was in fourth position. Figure 2 shows two typical examples of Z_{mouth} while the player is playing a low pitch note B♭2 and a mid-high pitch note F4, with the slide in first position. In this experiment, the transducer records simultaneously the response to the injected broadband current and the acoustic pressure caused by the vibrating lips. Consequently, the

harmonics of the note being played appear as narrow peaks superimposed on Z_{mouth} at the playing frequency and its harmonics. In order to estimate the position and the level of the vocal tract impedance peaks, these sharp peaks were discarded using a Savitzky–Golay smoothing filter of order 3 (Savitzky and Golay, 1964), to give the impedance spectra shown in Fig. 2. The magnitude of the bore impedance is displayed on the same figure, as well as the playing frequencies while playing the notes B♭2 and F4.

All impedance spectra measured in the mouth feature two broad peaks in the frequency range from 50 to 900 Hz. The curves displayed in Fig. 2 have similar overall shapes for both notes B♭2 and F4. For all players, the peaks in Z_{mouth} are about 10 to 30 times smaller than those in Z_{bore} around the playing frequency of the notes studied.

Figure 3 compares the playing frequencies and their harmonics with the frequencies of the first two peaks of Z_{mouth} and with the nominal frequencies of the equal tempered notes played relative to the standard 440 Hz. For each player, the first vocal tract impedance peak is always located between 200 and 325 Hz and does not change with the playing frequency.

As shown in Fig. 3, the measured frequencies of the first two vocal tract impedance peaks (resonances) vary little with the pitch played and show no obvious relation to the playing frequency and its multiples. All the players in this study played from the low (B♭2) to mid-high pitch notes (F4), without tuning the impedance peaks of their vocal tract.

The impedance maximum around 200 Hz requires discussion, because at this frequency the vocal tract length is about one tenth of a wavelength. In a simple model (Hanna *et al.*, 2012), the tract is approximated as a pipe of uniform cross section with length 16 cm and with radius 14 mm. At frequencies for which the tract's dimensions are small
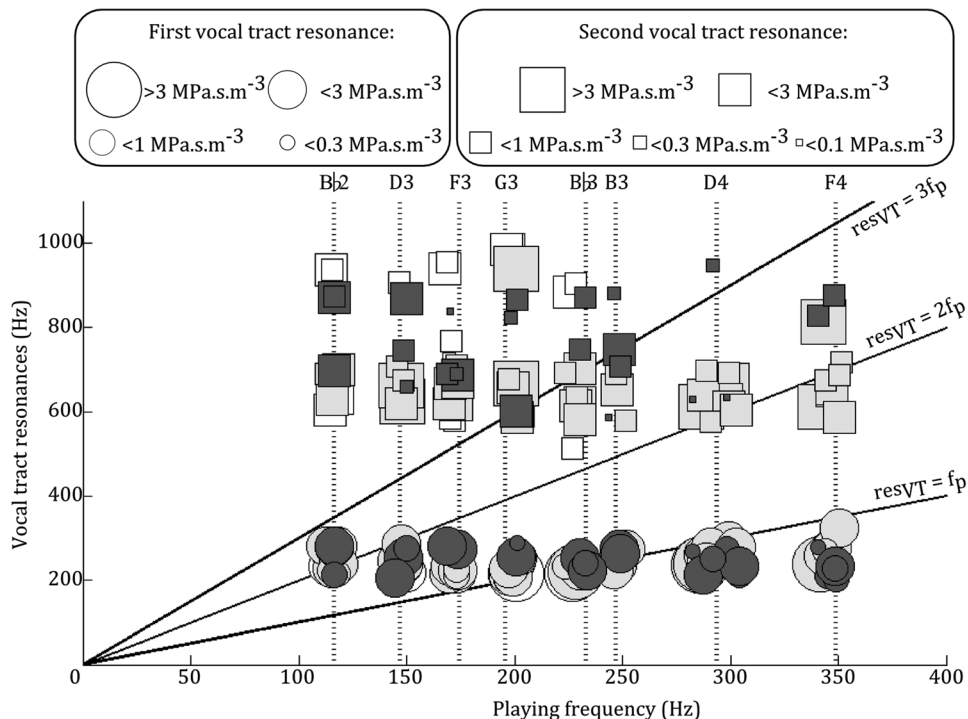

FIG. 3. Frequency of the first two maxima in the vocal tract impedance Z_{mouth} (resonances) compared with the playing frequency and the next two harmonics. The open symbols are data for beginners, the shaded symbols for amateurs and the darkest for professionals. The magnitudes of the first and second measured maxima of Z_{mouth} are binned in half decades, as shown in the legend and depicted by circles and squares, respectively. The three solid lines indicate when the vocal tract impedance peaks res_{VT} would be equal to the playing frequency f_p, and its harmonics $2f_p$ and $3f_p$. The dotted vertical lines indicate the nominal frequencies of the notes played.

compared with the wavelength, it is approximated as an acoustically compact object. The non-rigid wall is modeled by a uniform vibrating mass m supported by a spring of constant k. Acoustically, the wall of the tract, of area A, appears as an inertance $L_t = m/A^2$ in series with the compliance $C_t = A^2/k$ associated with deformability of the tissue surrounding the tract. Thus, at low frequencies, the impedance head at the lips measures this series impedance in parallel with the acoustic compliance C_{air} of the air in the tract. Approximate values of these parameters were determined by Hanna *et al.* (2012) by fitting measurements of vocal tract impedances: $C_{air} = 7 \times 10^{-10}$ m^3 Pa^{-1}, $L_t = 900$ kg m^{-4}, and $C_t = 7 \times 10^{-8}$ m^3 Pa^{-1}.

When the glottis is closed, these values predict a first maximum of Z_{mouth} at a frequency given by $1/(2\pi\sqrt{L_t C_{air}})$ ≈ 200 Hz. When the glottis is open, the trachea is connected and the subglottal airway can be approximated as a rigid-walled uniform pipe with length 20 cm and same radius as the tract, opened at its far-end (Lulich *et al.*, 2011). Consequently when the glottis is open, the first maximum of Z_{mouth} has a higher frequency since the vocal tract is partly open at its far-end. Further, for a glottis with an effective length of 2 cm (including end effects), as the glottal aperture becomes wider, the frequency of this maximum increases and reaches 290 Hz when the glottal radius is 1 cm, i.e., slightly below the subglottal effective radius. This value is dependent on the geometric parameters chosen, which would vary somewhat among players.

This model is consistent with the measured range of the first peak of Z_{mouth} and shows that a larger glottal aperture tends to raise its frequency. Further, according to this model, the players can adjust this resonance frequency only over a range that is less than 100 Hz, which may partly explain why they do not tune the first peak to play the notes in this study.

The measurements of the second peak of Z_{mouth} are spread over a wider range than the first, between 513 and 985 Hz. At these frequencies, the tract length is comparable with a half wavelength, so frequencies of the peaks depend strongly on the detailed geometry, and can presumably be modified by varying the position and shape of the tongue, as is done in speech to vary the resonances of the tract in the upper end of this frequency range. As shown in Fig. 3, the measured values split in two groups, one centered around 650 Hz and the other around 900 Hz, with standard deviations of 53 and 48 Hz, respectively. The second impedance peak was more often in the higher frequency group for beginners (41% of the notes played) than for advanced players (18% of the notes).

The average magnitudes of the first two impedance peaks of the vocal tract for all players are, respectively, 1.6 and 1.3 MPa s m^{-3}. According to the simple model of the vocal tract cited above, a narrower glottal aperture would increase the subglottal inertance. Then the frequency of the first two peaks of Z_{mouth} would decrease, as well as the amplitude of the second one. These variations are consistent with the observation by Mukai (1992) that experienced players have a narrower glottis than beginners, and with the statements by the professional players in this study, that they are playing with vocal folds almost closed. Using this model of the glottis, a reduction of the aperture also increases the

amplitude of the first impedance peak, and this variation is about ten times smaller than the amplitude reduction of the subsequent peak. However the amplitude of the first peak also depends on the geometry of the vocal tract, and that could explain why this variation is not shown by the measurements in Fig. 3.

The first seven peaks of Z_{bore} have magnitudes between 17 and 26 MPa s m^{-3}. Thus, for the series of notes from B♭2 to F4, since the performer played near these resonances, Z_{bore} was always much larger than Z_{mouth} (see Fig. 2). For notes above this range, the bore impedance peaks are reduced and become comparable with those in Z_{mouth}; the acoustic pressure in the mouth can then approach or exceed that in the bore (as measured by Fréour and Scavone, 2013).

Compared with beginners, advanced trombone players use a lower frequency second peak of their vocal tract impedance. Players in the present study showed no tendency to tune either the first or the second impedance peak to the note played or to one of its harmonics. A comparable experiment on trumpet players, extending into the *altissimo* range of that instrument, also found no tuning (Chen *et al.*, 2012). In the next section, the relationship between the playing frequency, Z_{bore} and Z_{mouth} is investigated in more detail.

B. Bore impedance at the playing frequency

In the second part of the experiment, the pressure in the mouth was measured while the player played ascending harmonic series with the slide in first and fourth positions. For each note, 32 samples of 1.5 s duration each were recorded. Samples measured when the player was inhaling were discarded. The playing frequencies of the other samples were estimated by the frequency of the narrow peak in the pressure spectrum caused by the vibrating lips. Their average values and standard deviations are shown in Fig. 4.

For 85% of the samples played by all players and 88% of the samples played by professionals, the fundamental playing frequency was above the closest peak of Z_{bore} (by 1.1% on average).

In a later experiment, four amateur and professional players were asked to play a note, to decrease ("lip down") and then to increase ("lip up") the pitch continuously, starting from F3 and from B♭3. For both notes, all four players reported they could lip down from their normal playing pitch over a bigger extent than they could lip up. This is confirmed by the measurements: they could play over a range between 12.1% below and 8.1% above the normal playing frequency of F3, and between 10.0% below and 8.9% above that of B♭3 (dashed horizontal bars and gray areas in Fig. 4). This experiment shows that the players are able to play continuously from one side to the other of the resonances, and thus play with downstream reactances of either sign. For normal playing, the bore impedance is almost always compliant. However, for all the notes studied, the lip oscillation can also be maintained while Z_{bore} is inertive.

For all notes studied here, at the average playing frequencies, the magnitude of the bore impedance is between 15.5 MPa s m^{-3} (when F4 is played with the slide in fourth position) and 22.9 MPa s m^{-3} (when D4 is played with the
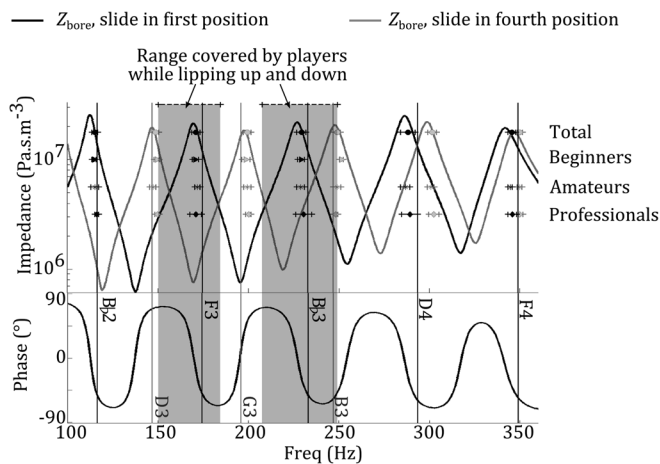
FIG. 4. The relationship between playing frequencies and the frequencies of impedance peaks of the bore. The black curve and gray curves are the measured bore impedance spectra for first and fourth positions, respectively. For each note, the average playing frequency produced by the professional players, the amateurs, the beginners, and all players are shown in different rows. The solid horizontal bars show the range for normal playing. The vertical solid lines indicate the nominal frequencies of the notes played. The dashed horizontal bars and the gray areas show the frequency range covered by advanced players while lipping up and down from F3 and B♭3. The black curves (magnitude in the upper part and phase in the lower part) give the magnitude and phase of Z_{bore}. (For clarity the phase is only shown for the first position.)
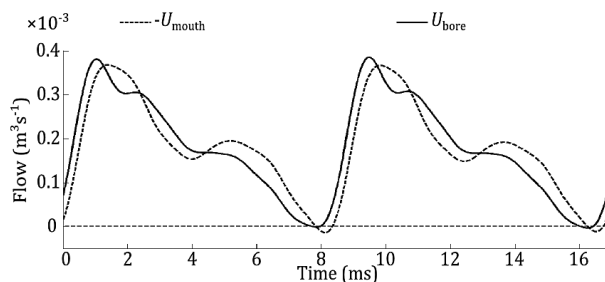

FIG. 5. Total flows calculated upstream (dashed) and downstream (solid) of the lip valve. Measurements were made simultaneously while the note B♭2 was played.

slide in first position). These values are more than ten times larger than the first two peaks of Z_{mouth} at the average playing frequencies. A simple model from Elliott and Bowsher (1982) and Benade (1985) approximates the lip valve as being driven by the difference of total pressure $\Delta P = P_{mouth} - P_{bore}$. Due to flow continuity, the flow into the mouth and that into the bore have opposite signs, but the same absolute values: $U_{mouth} = -U_{bore} = U$. For the notes in this study, $Z_{mouth} \ll Z_{bore}$ at the playing frequency, so variations in the mouth impedance have little impact on the series acoustic load acting on the lips.

C. Time domain

In order to investigate the operation of the lip valve, the pressure and components of the flow on either side of the lip valve are measured, or calculated from the measured data, and compared in the time domain, along with the lip aperture A_{ch}, and the horizontal and vertical deflections of the lips.

The acoustic flows in the mouth and in the mouthpiece are calculated from the ratios of the measured acoustic pressure to the measured impedance. The sign of the flow in the mouth was reversed so that the flow traveling from the mouth to the lips is positive.

Measuring the impedance in the bore is straightforward, but measuring it in the mouth during performance has technical challenges. A check on the method is to compare the total up- and down-stream flows, which are expected to be close to equal in the absence of experimental artifacts. Figure 5 shows these flows, U_{bore} and $-U_{mouth}$, determined using the configurations shown in Fig. 1(B) and Fig. 1(C). To measure Z_{mouth}, the sharp peaks due to harmonics of the played note were discarded and the data smoothed with a

Savitzky–Golay filter of order 3. The waveforms were obtained by averaging 21 consecutive groups of two cycles that overlapped their predecessor by one cycle. The results are shown in Fig. 5 for the low note B♭2.

The ac (alternating current) components of the waveforms are similar in magnitude and phase, and the overall shapes are reassuringly similar. However, they are not exactly equal, as required by continuity if all flow from the mouth goes into the instrument bore. It is possible that some flow leaks past the impedance head placed in the corner of the player's mouth. (A small flow could also enter it.) This might contribute to the differences in amplitude of the high frequency components in the waveform. The differences in shape may also be the result of the low pass filtering to remove noise in the measurements of Z_{mouth}. Consequently, the measurements of flow out of the mouth must be considered as approximate rather than precise measurements. The measured average flow in our experiments was 140–250 mL s^{-1}, which falls in the range measured for relatively quiet playing by Bouhuys (1968) and by Fréour et al. (2010) in the case of the trumpet.

Figures 6 and 8 show examples of the waveforms measured on the same advanced player. As shown in Fig. 1, the high-speed video and the upstream acoustic pressure p_{mouth} were measured separately using different experimental configurations. However, the downstream acoustic pressure p_{bore} was recorded in both experiments and displayed on an oscilloscope so that the performer could play at the same amplitude and frequency. The acoustic pressure in the mouth was synchronized with the mouthpiece pressure and the video. For this particular player, the dc pressure in the mouth called $\bar{p}_{mouth}$ was also measured simultaneously in both experiments using a pressure gauge. The steady excess pressure in the mouthpiece as recorded by the pressure transducer was close to zero. Thus the total pressures $P_{mouth} = \bar{p}_{mouth} + p_{mouth}$ and $P_{bore} \approx p_{bore}$ can be plotted together; for a low pitch note, B♭2, see Fig. 6(A), and a mid-high pitch note, F4, see Fig. 8(A).

The acoustic flow u_{bore} was deduced from the pressure and the impedance measured in the mouthpiece cup, see Sec. II C 2. The steady flow was estimated with the method described in Sec. II C 4. The sum of these components gives the total flow downstream of the lip valve. Also plotted is a component of the total flow: the sweeping flow due to the air displacement generated by the lips, which is calculated using the method of Sec. II C 3, cf. Figs. 6(B) and 8(B).
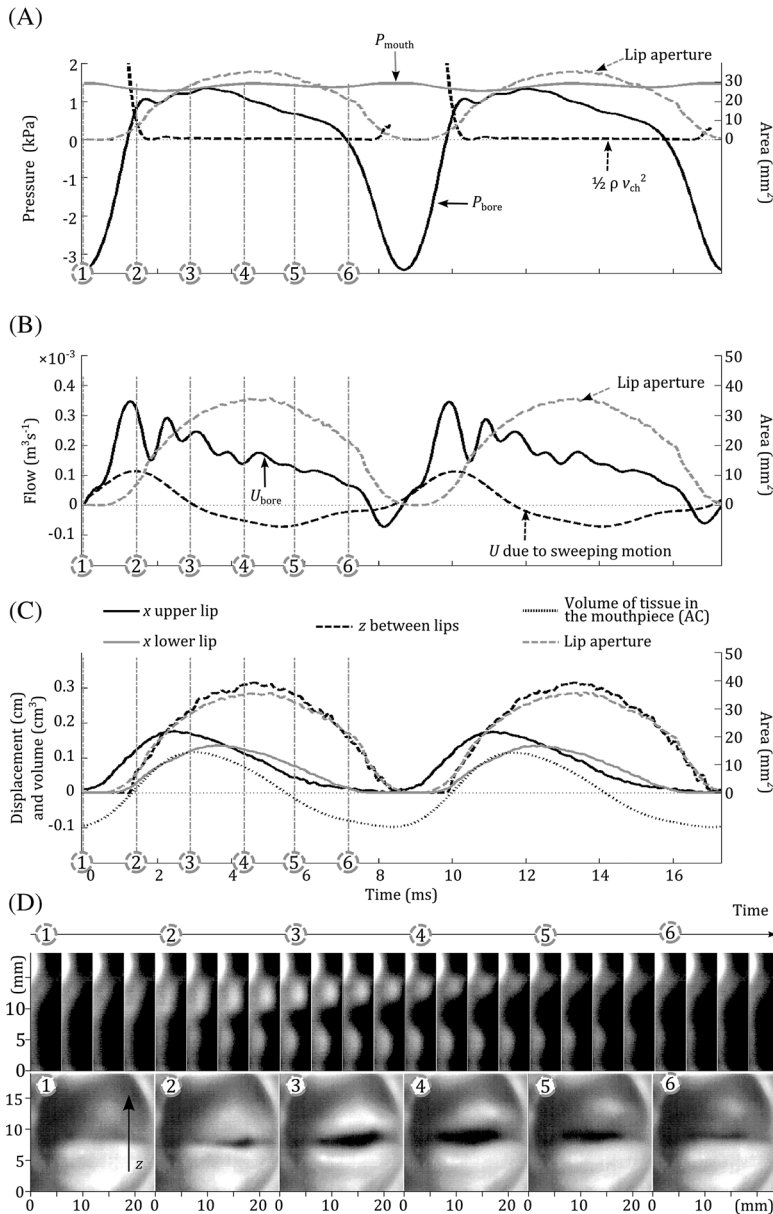
FIG. 6. The note played is B♭2. The top graph (A) shows the upstream (solid gray) and downstream (solid black) pressures and the Bernoulli term (dashed black) defined as $\rho v_{ch}^2/2$, where ρ is the air density and v_{ch} is the speed of air in the lip channel. The next (B) shows the total flow (solid black) and the swept flow (dashed black) due to the lip motion *per se*. The third (C) shows the longitudinal motion of the upper (solid black) and lower (solid gray) lips, the vertical separation between them (dashed black), as well as the alternating component of the volume of tissue in the mouthpiece cup (dotted black). On all these graphs the dashed gray curve shows the lip aperture. The fourth graph (D) shows the motion of the lips during one cycle filmed with high-speed video. The top sequence is the side view and the bottom sequence the front view. On the curves of (A), (B) and (C), the numbers identify the six video frames of the front view.

As shown in the side views of the video sequences of Figs. 6(D) and 8(D), on each lip, the points of the front edge do not oscillate in phase. The average horizontal deflections, $\hat{x}_{up}$ and $\hat{x}_{low}$, and the vertical separation between the lips, z, are calculated using the method of Sec. II C 5, and plotted in Fig. 6(C) and Fig. 8(C) together with the volume of tissue in the mouthpiece.

The lip aperture A_{ch} is determined using the front view of the video (see Sec. II C 1). It is displayed on each subfigure, in order to allow comparisons between the phase and the magnitude of all the waveforms while the performer plays a low pitch note (B♭2), see Fig. 6, and a higher note (F4), see Fig. 8.

In previous models (e.g., Elliott and Bowsher, 1982; Fletcher, 1993), the inertive reactance of the air in the lip channel was usually assumed to be negligible compared to the input impedance of the bore at the playing frequency. Further, it is often assumed that the flow from the mouth to the lip channel is laminar, but that the jet leaving this aperture is turbulent and that its kinetic energy is dissipated in the mouthpiece cup. Subject to that simplification, there is no recovery in pressure across the turbulent region and pressures in the channel and

the mouthpiece are approximately equal. It is also often assumed that the flow passing between the lips is always forward: i.e., that the dc flow is greater than the negative amplitude of the acoustic flow. With these assumptions, and with $P_{bore} \approx p_{bore}$, Bernoulli's equation gives

$$P_{mouth} - p_{bore} = \frac{\rho}{2}\left(v_{ch}^2 - v_{mouth}^2\right), \tag{1}$$

where v_{mouth} is the speed of the jet at the impedance head just inside the mouth, v_{ch} that inside the channel, and ρ is the density of the air. The cross section is much larger in the mouth than in the channel. Then, Eq. (1) becomes

$$P_{mouth} - p_{bore} = \frac{\rho}{2} U_{ch}^2/A_{ch}^2, \tag{2}$$

where U_{ch} is the flow in the lip channel, which is expected to equal the flow out of the mouth and that into the mouthpiece. In principle, the measured waveforms allow the calculation of the right hand side of Eq. (2), henceforth called Bernoulli term. It is plotted together with P_{mouth} and p_{bore}, cf. Figs. 6(A) and 8(A). However, the Bernoulli term can only be considered
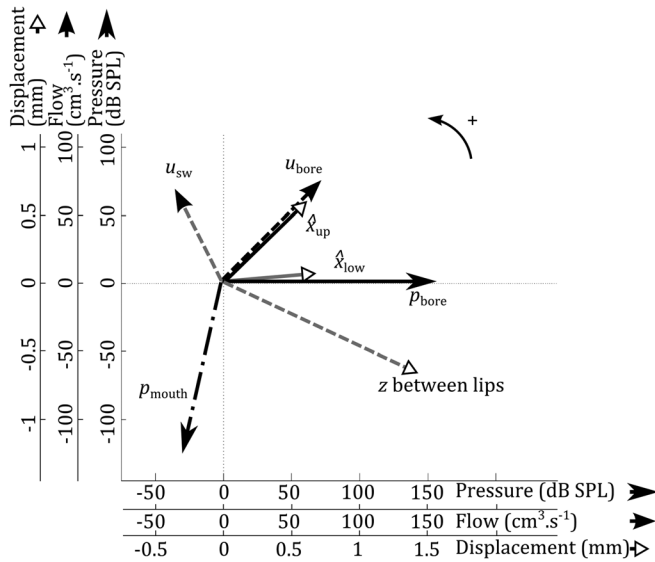
FIG. 7. Phasor diagrams of the fundamental frequency components of the upstream and downstream pressures, the flow into the mouthpiece, the sweeping flow due to the lip motion, the longitudinal displacement of the upper and lower lips and the vertical separation between the lips. The angles between the arrows give the phase differences between the components, with the phase of the mouthpiece pressure taken as the reference. Phase increases in the positive (anticlockwise) direction, so the sweeping flow leads in phase. The note played is B♭2.

as an order-of-magnitude estimate, for two reasons. First, there are the non-negligible experimental uncertainties mentioned above in obtaining the total flow. More importantly, the sensitivity to errors in A_{ch} in Eq. (2), which appears squared in the denominator, is greater when A_{ch} is small, which is also the only time when the Bernoulli term is large.

Figures 6(D) and 8(D) are composed of regularly spaced sequences of six front views and of 24 side views, illustrating the motion of the lips during one oscillation cycle. The instants corresponding to each of the front views are specified by numbers 1–6 on the subfigures (A), (B), and (C).

1. Low pitch note B♭2

The first note studied, B♭2, is the lowest pitch note that can be produced with the slide in first position (not counting the pedal note, for which the fundamental frequency is not near an impedance peak). The measurements were segmented into synchronized groups of two cycles overlapping their predecessor by one cycle. The plotted waveforms were obtained by averaging 21 consecutive groups with constant amplitude and frequency.

The pressure waveforms in Fig. 6(A) illustrate the strongly nonlinear behavior of the lip valve. The dc pressure, equal to 1.4 kPa in the mouth with an error less than 10%, is assumed to be near zero in the mouthpiece cup, while the amplitude of its alternating pressure component is 20 times larger in the mouthpiece than in the mouth. A large negative pressure in the mouthpiece occurs when the lips are closed. During this closed phase, this large negative mouthpiece pressure is at least largely involved in producing the acceleration that converts the backwards motion of the lip into forwards motion in the next cycle.

P_{mouth} displays two local maxima per cycle. This was observed with all performers. In this example, the second harmonic of P_{mouth} exceeds the first by 3.6 dB, while for

P_{bore}, the second harmonic is smaller by 5.2 dB. The double maxima are a result of the broad first peak in Z_{mouth} falling in the vicinity of the second harmonic for this note.

During the first half of the lip-open phase, it is observed [Fig. 6(A)] that P_{mouth} is close to the sum of P_{bore} and the Bernoulli term. This is what would be expected if the inertance of and aerodynamic losses in the air in the channel were negligible. In the second half of the open phase, there is a substantial difference between the up- and down-stream pressures, and the difference exceeds the Bernoulli term. It is difficult to explain this difference with plausible values of inertance and aerodynamic loss. Part of the explanation may be the sensitivity of the Bernoulli term to errors, as discussed above.

While the Bernoulli term is difficult to calculate, it is potentially important because of its possible effect in driving the vertical motion of the lips. While the lips are closed, there is no flow between them so the Bernoulli term must be zero. However, the calculated Bernoulli term has very high values just after the lips separate and before they meet, because the lip aperture is small, and the flow through the channel is not zero. During the rest of the opening phase, the aperture is large, so the velocity is relatively small and the Bernoulli term is close to zero. As mentioned above, the values plotted for this term are rough estimates only.

The total flow into the bore starts to rise before the lips separate, because of the longitudinal or sweeping motion of the lips. While the lips are closed, the total flow into the bore and the swept flow must be equal, and the measurements in Fig. 6(B) are approximately equal. Then, during the lip-open phase, the difference $U_{bore} - u_{sw}$, which is equal to the flow through the lip channel, first increases and then decreases. Figure 6(B) shows that, for this low note, the peak to peak amplitude of the sweeping flow is 180 cm^3 s^{-1}, which is a considerable fraction of the total flow, whose peak to peak amplitude is about 400 cm^3 s^{-1}. We notice that, for this player, the total flow into the bore is briefly negative. Further, during this phase the sweeping flow is small, so the calculations in this example suggest a small, brief flow going between the lips back into the mouth. However this feature was not systematically observed for all players and all notes.

The lip aperture and the vertical separation between the lips are almost exactly in phase. Further, their ratio varies very little over the cycle, between 1.1 and 1.5 cm, which is approximately the width of the aperture. The average horizontal displacement of the upper lip, $\hat{x}_{up}$, leads that of the lower lip, $\hat{x}_{low}$, which in turn precedes the vertical separation z. For seven subjects playing B♭2, including one beginner, the leading lip, i.e., the one ahead in phase, is the upper one, while it is the lower one for only two players, including one beginner. The lower lip of the third beginner had no noticeable oscillation. The horizontal deflection of the leading lip for all subjects was always ahead of z. For eight of the nine subjects, the following lip was also ahead of z.

In the sequence of Fig. 6(D), the front view shows that the upper lip motion is not symmetric about the z axis crossing the lip center. The same asymmetry was observed by Copley and Strong (1996), Yoshikawa and Muto (2003), and Bromage et al. (2010) in the case of trombone and French horn players producing low pitch notes.
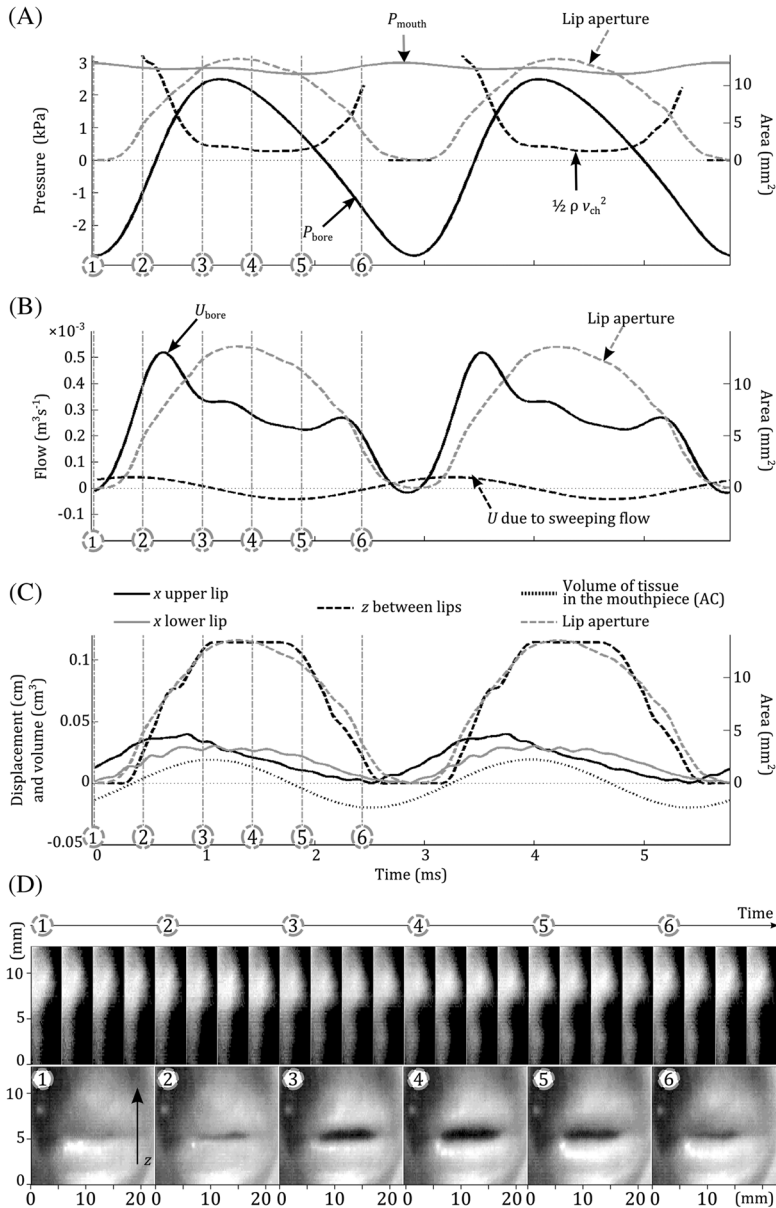
FIG. 8. The note played is F4. The top graph (A) shows the upstream (solid gray) and downstream (solid black) pressures and the Bernoulli term (dashed black) defined by $\rho v_{ch}^2/2$ where ρ is the air density and v_{ch} is the speed of air in the lip channel. The next (B) shows the total flow (solid black) and the swept flow (dashed black) due to the lip motion *per se*. The third (C) shows the longitudinal motion of the upper (solid black) and lower (solid gray) lips and the vertical separation between them (dashed black), as well as the alternating component of the volume of tissue in the mouthpiece (dotted black). On all these graphs, the dashed gray curve shows the lip aperture. The fourth graph (D) shows the motion of the lips during one cycle filmed with high-speed video. The top sequence is the side view and the bottom sequence is the front view. On the curves of (A), (B), and (C), the numbers identify the six video frames of the front view.

Figure 7 is a phasor diagram: the length of each arrow represents the magnitude while its angle above the x axis shows the phase with respect to the mouthpiece pressure. This diagram shows the fundamental frequency components of the lip motion, the flow into the mouthpiece, the sweeping flow and the pressures on either side of the lip.

As previously commented, the sweeping flow (u_{sw}) is ahead of the total flow in the mouthpiece, which is in turn ahead of z and consequently the lip aperture. The sweeping flow must be ahead of the volume of tissue within the mouthpiece by 90°, since it is equal to its time derivative. The cross-section of the portion of lips in the (x, z) plane is equal to $h_{up}\hat{x}_{up} + h_{low}\hat{x}_{low}$, h_{up} and h_{low} being the effective lengths of the upper lip and the lower lip, respectively. This cross-section is also equal to the volume of tissue divided by the effective width of the aperture, so that it must be in phase with this volume. Consistent with this, the horizontal deflections of the upper and lower lips lag behind u_{sw} by 73° and 113°, respectively. The measured ratio of 1.2 between the

fundamental components of $\hat{x}_{up}$ and $\hat{x}_{low}$ allows estimation of the ratio between the effective lengths of the upper and lower lips,

$$\frac{h_{low}}{h_{up}} = \frac{\hat{x}_{up}}{\hat{x}_{low}} \times \frac{\sin(90° - 73°)}{\sin(113° - 90°)} = 0.9. \tag{3}$$

This result is a rough estimate since it only considers the longitudinal deflections at the fundamental frequency. For the other players, the same calculation gives values of h_{low}/h_{up} between 0.4 and 0.9 and shows that the upper lip has the larger effective length while playing B♭2.

Since the total flow in the mouthpiece cup is ahead of the pressure, the bore impedance is compliant at the playing frequency for the example given in Figs. 6 and 7. From Fig. 4 this is not surprising, since most of the B♭2 notes were played above the first bore resonance.

The pressure in the mouth lags behind that in the mouthpiece. However, since the second harmonic of p_{mouth} is larger than the fundamental, the phasor diagram does not

allow prediction of the relative position of the maxima of p_mouth and p_bore observed on Fig. 6(A).

2. Higher pitch note F4

The second note studied in detail, F4, allows the investigation of the lip motion in a rather higher part of the range. F4 is the fifth note (above the pedal note) of the ascending harmonic series played with the slide in first position. As in Fig. 6, the measurements were segmented into synchronized groups of two cycles overlapping their predecessor by one cycle. The plotted waveforms of Fig. 8 are averages of 43 consecutive groups with constant amplitude and frequency.

Again, when the lips are open, we observe that the mouth pressure P_mouth is similar to the sum of the mouthpiece pressure P_bore and the Bernoulli term, where the Bernoulli term is greater than in the low note. The inertia of the air in the channel, which is larger at higher frequency, also possibly contributes to the pressure difference $P_\text{mouth} - P_\text{bore}$. As for the low note, the large negative mouthpiece pressure occurs when the lips are closed.

For this higher note, the period during which the lips are closed is reduced to 6% of the cycle (compared with 10% for B♭2). Consequently, the lip aperture waveform becomes more sinusoidal, as do the other waveforms. In particular, compared to the low pitch note, the second harmonics of P_mouth and P_bore are significantly decreased, going from 3.3 dB above and 5.0 dB below the fundamental to 3.0 and 14.0 dB below the fundamental.

In Fig. 8(D), the side view shows that the motion of the lips is predominantly vertical. This is confirmed by the amplitude ratio of longitudinal and vertical components (35% for the upper lip and 26% for the lower lip), which are significantly reduced compared with those of B♭2 (56% for the upper lip and 43% for the lower lip). Consequently, the relative contribution of swept flow in U_bore is rather smaller for F4 than for B♭2. This explains why U_bore is close to zero when the lips are closed, see Fig. 8(B). In addition, the amplitude of the volume of tissue in the mouthpiece, 40 mm³, is reduced by a factor of 5.3 compared to B♭2, 210 mm³.

Again the lip aperture is in phase with the vertical separation between the lips and their ratio has small variation over the cycle, between 1.1 and 1.3 cm. Thus the aperture width is still approximately constant while the lips are open, as observed by Copley and Strong (1996), but its value is slightly reduced compared to B♭2, as observed by Bromage *et al.* (2010).

From the front view of Fig. 8(D), the motion is more symmetric about the z axis crossing the lip center than for B♭2.

The phasor diagram of Fig. 9 allows comparisons among the amplitudes and phases of the fundamental components of the longitudinal and vertical deflections, the flow into the mouthpiece and the pressures up- and downstream of the lip valve, as well as the swept flow due to the lip motion.

For F4, the longitudinal components of the lip motions are significantly smaller than the vertical separation between the lips, while they have the same order of magnitude for B♭2. The qualitative phase relation among $\hat{x}_\text{up}$, $\hat{x}_\text{low}$, z, and p_bore is unchanged. The beginners could not play F4. Among the six players who could play it, the same relation of phase
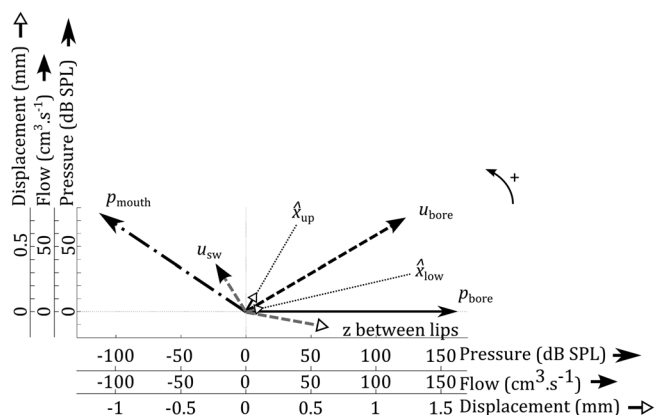

FIG. 9. Phasor diagrams of the fundamental frequency components of the upstream and downstream pressures, the flow into the mouthpiece, the sweeping flow due to the lip motion, the longitudinal displacement of the upper and lower lips and the vertical separation between the lips. The angles between the arrows show the phase differences between the components. The phase of the mouthpiece pressure is taken as the reference. The note played is F4.

among the x-deflection of the leading lip, p_bore and z is observed for two professional and one advanced player. For the other players, p_bore is ahead of the deflections: z precedes $\hat{x}_\text{up}$ for one professional and one advanced player and lags behind $\hat{x}_\text{up}$ for one advanced player.

For the advanced player involved in the examples shown in Figs. 7 and 9, comparing the measurements for F4 with those for B♭2, the deflections $\hat{x}_\text{up}$, $\hat{x}_\text{low}$, and z have moved ahead (anticlockwise) by 16°, 7°, and 14°, respectively, relative to p_bore. However, for all the other players involved in the study, z lags further behind p_bore while playing F4, and for all the other players except one professional, $\hat{x}_\text{up}$ also lags further behind p_bore while playing F4. While the phase relation between the deflections and p_bore is consistent among players in the lower range, it appears that different regimes of oscillation may be possible in the higher range, involving various possible phase relations.

In the example shown, u_bore is ahead of p_bore. Thus, Z_bore is compliant at the playing frequency. This is in agreement with the impedance curve of Fig. 4 showing a negative slope at 349 Hz, the frequency of F4.

Last, the volume of tissue in the mouthpiece cup (not plotted in Fig. 9) is by definition 90° behind u_sw. This volume is 21° ahead of $\hat{x}_\text{low}$, and 28° behind $\hat{x}_\text{up}$. Equation (3) gives an estimate of the ratio between the heights of the lips: $h_\text{low}/h_\text{up} = 1.7$. The extension of the lower lip relative to the upper lip, compared to the low note, is probably achieved by lowering the mouthpiece. For the other players, the longitudinal vibration of the lower lip was not significant so that this ratio could not be calculated.

D. Phase relations of the *x* and *z* motions

Copley and Strong (1996) published diagrams of the trajectory measured at a central point of player's upper lip during playing. Later Yoshikawa and Muto (2003) measured 2D-trajectories of the upper lip tip as well as the crest of the wave traveling along the upper lip surface. In this study, similar phase diagrams show the vertical separation between the lips as a function of the longitudinal deflection of the leading

J. Acoust. Soc. Am., Vol. 137, No. 3, March 2015

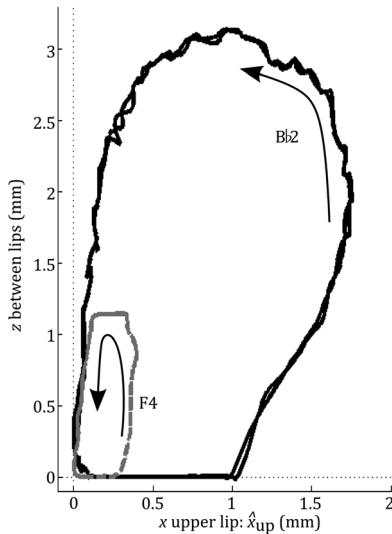Boutin *et al.*: Acoustic flows during trombone playing 1205

FIG. 10. Phase diagrams showing the vertical separation between the lips as a function of the average longitudinal deflection of the upper lip, while the performer is playing B♭2 (solid black) and F4 (dashed gray). For each note, two cycles are displayed. The smallest value reached by each component is defined to be zero.

lip for both notes B♭2 and F4, see Fig. 10. The measurements shown are the two averaged cycles, $\hat{x}_{up}$ and z, plotted in Figs. 6(C) and 8(C).

Both trajectories are anticlockwise, as was observed by Copley and Strong (1996), and Yoshikawa and Muto (2003). In addition this diagram shows that for F4, $\hat{x}_{up}$ is reduced by a factor of about 4 and z by about 3 compared to B♭2.

IV. DISCUSSION

A. Models of the lip valve

Helmholtz (1877) distinguished between two kinds of valve mechanisms that occur at the input of wind instruments. The inward-striking valves are closed by a positive pressure difference between the mouth and the mouthpiece, while the outward-striking valves are opened by such a pressure difference. With a simple one-degree-of-freedom model, Fletcher (1993) showed that the oscillation of an outward-striking cantilever beam will auto-oscillate at a frequency higher than both its natural frequency and that of the nearest bore resonance. However, subsequent experimental studies (Yoshikawa, 1995; Chen and Weinreich, 1996; Campbell, 1999) showed that brass players could play above or below the frequencies of the bore resonances, when the acoustic loads are compliant or inertive. We return to discuss "lipping down" and inertive loads below.

Cullen et al. (2000) draw attention to the importance of multimode oscillation in regenerative models of brass players' lips. The two-mass models of vocal folds proposed by Ishizaka and Flanagan (1972), Pelorson et al. (1994), and Lous et al. (1998) explain auto-oscillation under a range of loads. However, the oscillations in these models are purely transverse: there is no sweeping flow, so they do not describe the lip motion observed here. Strong and Dudley (1993) and Adachi and Sato (1996) propose models that involve both a

swinging action, which produces sweeping flow, and a compression along the length. By solving their equations of motion numerically, Adachi and Sato show that these models can produce autonomous oscillations below and above the bore resonances.

The images in Fig. 6(D) show that the upper lip undergoes a swinging motion in the (x, z) plane, an oscillation of length in the z direction (as in the Adachi and Sato model) and also bending in the (x, z) plane. In order to focus on the essential physics, the condition of auto-oscillation is discussed qualitatively below, first using a model close to that of Adachi and Sato, and then, separately, using another simplified model that represents the continuous bending of the real lip by the coupled motion of two plates.

The first model treats the lip as a compressible beam that can undergo shear and length contraction subject to a vertical spring, supplied by the elasticity of the tissue itself, and a horizontal spring, due to the elasticity and tension across the lip, as shown in Fig. 11 for the upper lip only. The beam is fixed at the top (AB). The two sine waves shown in the bottom sketch approximate the normalized average horizontal components $\hat{x}_{up}$ and separation between the lips $z = 2z_0$. Their phase difference has been chosen to be similar to that in Fig. 6(C), and the times (a), (b), (c), and (d) correspond approximately to the frames thus labeled in that figure. The motion of the lower lip (not shown) is nearly symmetrical with that of the top, reflected about the dashed line.

Flow separation at constrictions of variable aperture is a complicated topic (see, e.g., Hirschberg, 1995). In this highly simplified model, flow separation is assumed to occur at the bottom of the lip, so that the pressure between the lips is approximately P_2. Consider a case with constant P_1 and P_2 (such as a player "buzzing" a mouthpiece-sized ring at a frequency that does not correspond to a peak in Z_{mouth}). Between (a) and (b) the pressure difference does work $(P_1 - P_2)\Delta V_{ab}$ on the lip due to its swinging motion, where the volume ΔV_{ab} is represented approximately by the dark gray area in sketch (b). Between (c) and (d), the pressure difference does negative work, $(P_1 - P_2)\Delta V_{cd}$, where the negative volume ΔV_{cd} is represented approximately by the pale gray area in (d). Because the lip is shorter during retraction, $|\Delta V_{ab}| > |\Delta V_{cd}|$, so the work done $(P_1 - P_2)(\Delta V_{ab} + \Delta V_{cd})$ over a complete cycle would be positive. As an example, this work is equal to 0.60 mJ and then 0.57 mJ over the two cycles of B♭2 described in Fig. 6. At 117 Hz, this contributes a power of 68 mW. This extra work term distinguishes such models from the one-component "swinging door" models, in which auto-oscillation is only possible above the bore resonance.

Around a complete cycle, the springs do no work. However, if the net work done by the pressure difference is positive, it can compensate for mechanical energy losses in the lips. Although the 68 mW mentioned above is less than the acoustic power of the airflow modulated by the vibrating lips (about 100 mW in Fig. 6), it is probably not small compared with the mechanical energy per cycle stored in the lip vibration alone, and so may be significant contribution in overcoming the mechanical losses associated with that vibration. Thus a significant contribution to auto-oscillation appears to come from the fact that the lip is longer in its forward motion than in
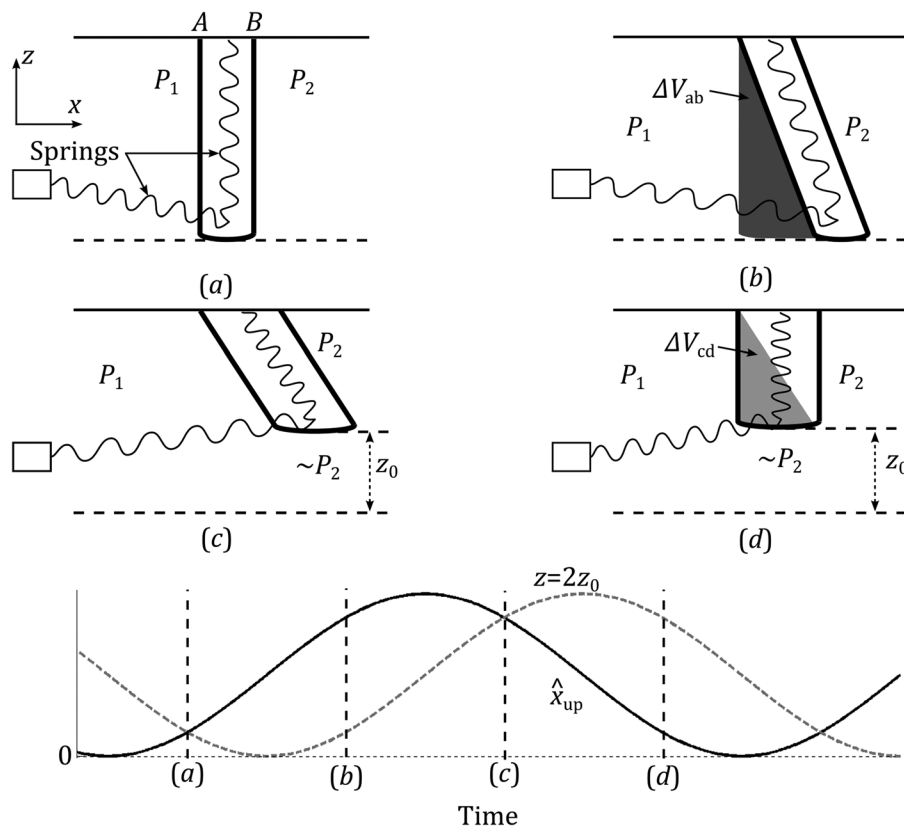
FIG. 11. A model of an upper lip with two degrees of freedom composed of a compressible beam, which undergoes both shear and compression-dilation. P_1 and P_2 are the pressure upstream and downstream of the valve, respectively, equal to P_{mouth} and P_{bore}. (The lower lip, not shown, would have a nearly symmetrical motion about the dashed axis.) The dark and light gray areas are approximate representations, respectively, of the positive and negative volume swept by the upper lip since the preceding sketch. The bottom graph shows sinusoidal approximations to the horizontal displacement (solid black) and vertical displacement (dashed gray).

the backward motion, i.e., that the horizontal component $\hat{x}_{up}$ for the upper lip and $\hat{x}_{low}$ for the lower lip leads the vertical separation z, as shown in Fig. 6(C). [It is worth noting that the volume swept due to this swinging motion is not equal to the sweeping flow plotted in Figs. 6(B) and 8(B) calculated from volume occupied by the lips, and for which the swept volume around a complete cycle is zero.]

Figure 6(D) shows another feature related to auto-oscillation that is not incorporated in the model just discussed: the motions of different parts of the lip do not have the same phase. This phase difference can also have the effect of making the lip longer during its forward sweeping motion and thus contributing to positive work being done around a complete cycle by the pressure difference. This is illustrated in Fig. 12, which pictures the upper lip as two rigid plates that can rotate at the upper limit and at their junction. The elasticity of the lip tissue is modeled by two torsion springs at points A and B. Again, flow separation is assumed at the bottom of the upper lip. For the purposes of qualitative discussion, the amplitudes of the rotation in this cartoon are arbitrarily set to $60°$ about zero for the upper beam and about $30°$ for the lower. The upper beam leads the lower by $135°$. These values were chosen to maximize the work done by the pressure difference.

During the first and the second halves of the cycle, (a–d) and (e–h), the upper plate sweeps the same area, so the work done on it by $P_{mouth} - P_{bore}$ is zero. In contrast, the lower plate draws different trajectories. Because of the positive offset of the angle β of the lower plate, the vertical position z_0 of the bottom-end of the model is smaller during the first half of the cycle, as in Fig. 11. Thus the effective length of the lips is longer while the upper plate moves forwards than backwards and the sum of the dark-gray area is larger

than the sum of the light-gray area over a complete cycle. Thus with $P_1 > P_2$, the work done by the pressure is positive and can compensate for losses because the torsion springs do no work over a complete cycle. For the upper plate to lead the lower in phase, its natural frequency would be higher. This is plausible for the real lip, because the "springs" in question are the tension of tissues in the y direction. The lips are fixed at the edge of the circular mouthpiece. This means that the lower part of the upper lip is longer in the y direction than the upper part. In turn, this effect alone makes the upper part a stiffer spring for deformation in the x direction.

In both of the above models, provided that the relative phase of the two oscillations is as indicated, a point on the leading lower edge of the top lip traces an anticlockwise path, in agreement with Fig. 10 and previous measurements (Copley and Strong, 1996; Yoshikawa and Muto, 2003). However, the motion shown in Figs. 6, 8, and 10 is more complicated than a combination of these two models. Nevertheless, the two effects suggest how auto-oscillation is possible in the absence of resonances. The effect of resonances is discussed next.

B. Models of lip valve connected to a downstream impedance

If one neglects the inertia of the air between the lips, and if flow separation occurs at the point of minimum aperture, then the pressure difference across the lips would be equal to the Bernoulli term during the phase when the lips are open. This is roughly what is seen in Figs. 6(A) and 8(A) during the early part of the open-lip phase. With only small variation in P_{mouth}, due to the small upstream impedance
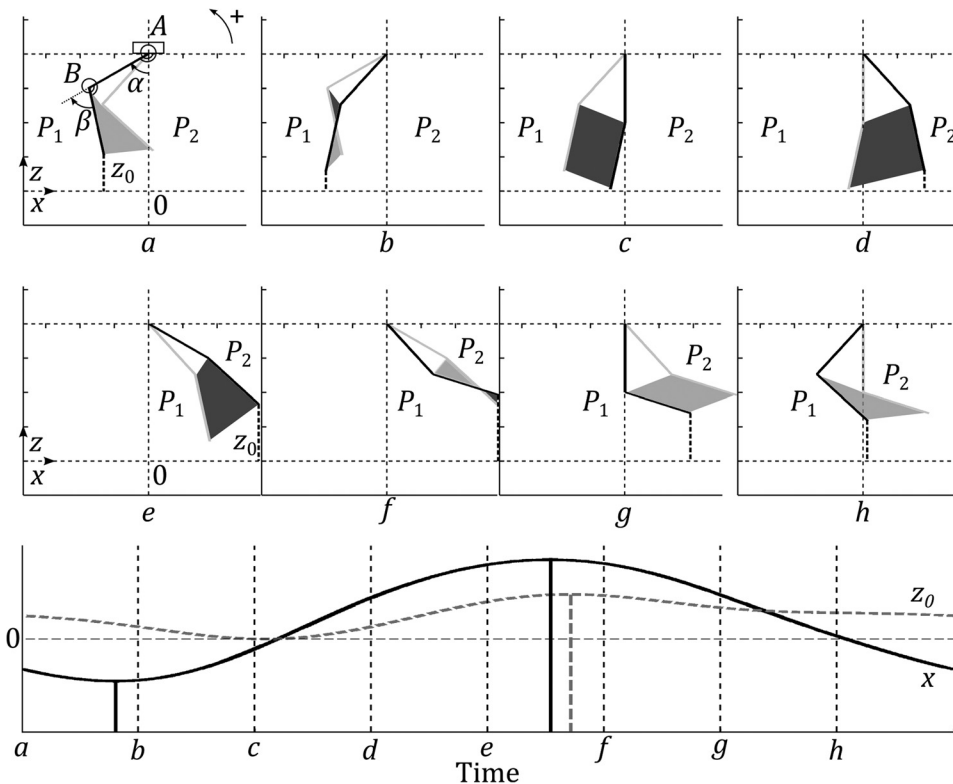
FIG. 12. Auto-oscillation with a flexible upper lip. A two-mass model comprises two connected rigid plates of fixed size, each in simple harmonic motion. In each sketch, the black line shows the current position and the pale line the previous position. The dark shading represents approximately the positive volume swept by the lower plate since the previous sketch, pale shading represents negative swept volume. Here, the phase of the upper plate leads that of the lower plate, with the result that the lip is vertically longer when traveling forwards than backwards. Hence the total swept volume is positive. The bottom graph shows the horizontal displacement x (solid black) and vertical displacement z_0 (dashed gray) at the lower end of the model lip.

and small values of the Bernoulli term while the lips are open, P_{bore} can only be large and negative during the phase while the lips are closed or while the lip aperture is very small, again approximately in agreement with Figs. 6(A) and 8(A). This phase also is observed to overlap substantially with the phase during which the lips move forwards. The work done by $P_{mouth} - P_{bore}$ is large when this pressure difference is large and positive during the forward motion of the lips. This makes the relation between the phase of the bore pressure and the sweeping flow and the phase and magnitude of the downstream impedance important in the energy balance of auto-oscillation. In consequence it is particularly interesting to understand how these phases vary when notes are lipped up or down over a large range. This was not measured here, but may yield interesting results in future studies.

V. CONCLUSIONS

For the low and medium pitch notes studied here, trombonists do not tune the vocal tract, whose impedance measured near the lips is much lower than that of the bore at playing frequencies. Consequently, Z_{mouth} has little influence on the series acoustic load ($Z_{mouth} + Z_{bore}$) acting on the lips. This is similar to the results found for trumpeters over a range extending into the *altissimo* (Chen *et al.*, 2012).

The measurements in this study plus high-speed video imaging allow simultaneous plotting of the motion of the lips in the (x, z) and (y, z) planes, the up- and down-stream pressure, the total flow into the mouthpiece and the component of that flow that is due to the sweeping motion of the lips.

These waveforms show that the mouth pressure is roughly equal to the sum of the mouthpiece pressure and the "Bernoulli pressure" term in the channel in the first part of the period where the lips are open. It confirms the usual assumption (e.g., Elliott and Bowsher, 1982) that the inertance of the air in the channel can be neglected for low and medium pitch notes. A puzzling discrepancy in the later part of the lip-open phase remains unexplained.

The measurements also reveal that the sweeping flow due to the longitudinal motion of the lips contributes substantially to the flow in the mouthpiece for the lower note Bb2, while its relative amplitude becomes smaller for the higher note F4.

From the lower to the higher note, the amplitudes of both longitudinal and transverse components of the leading lip trajectory are reduced by similar fractions. Further, these components of the motion and the flow all maintain qualitatively similar phase relations relative to the mouthpiece pressure. This suggests that the lip valve behavior varies continuously in this frequency range, rather than showing a distinct transition between mechanisms.

The trombone players were able to play both below and above the bore resonances, and to "bend" the note from one side to another without discontinuity. Therefore lip oscillation is possible for both compliant or inertive acoustic loads downstream of the lip valve and can be maintained while the nature of the load is changed.

The frequency range that could be reached by experienced players bending the pitch around F3 and Bb3 was approximately centered on the peak in the bore impedance and not on the normal playing frequencies of the notes, which lie above the impedance peaks. This feature, plus an asymmetry in the impedance peaks of the bore, could explain why the players reported that they can "lip down" further than they can "lip up" for these notes. Lip oscillation, whether with inertive or compliant Z_{bore}, occurs over a limited range in the difference between the bore resonance and

the playing frequency. Perhaps this is because the phase difference between the mouthpiece pressure and the flow must lie in a limited (positive or negative) range so to produce regeneration of the oscillation.

The observed motion of the lips combines some features of the one mass-two spring model of Adachi and Sato (1996), and some of a simple model using two masses, one above the other, with different phases. In both, some of the work required for auto-oscillation is produced because the effective length of the lip is shorter while moving backwards than forwards, so that a pressure excess upstream can do positive work on the sweeping motion of the lips and thus produce auto-oscillation over a range of load conditions, including small impedance on both sides, such as for a player "buzzing" the lips without a trombone.

ACKNOWLEDGMENTS

Adachi, S., and Sato, M. (**1996**). "Trumpet sound simulation using a two-dimensional lip vibration model," J. Acoust. Soc. Am. **99**, 1200–1209.

Ayers, R. D., and Lodin, M. S. (**2000**). "Alternative mouthpiece design for viewing the lip reed in motion," J. Acoust. Soc. Am. **107**, 2843.

Backus, J. (**1976**). "Input impedance curves for the brass instruments," J. Acoust. Soc. Am. **60**(2), 470–480.

Benade, A. H. (**1976**). *Fundamentals of Musical Acoustics* (Oxford University Press, New York), p. 393.

Benade, A. H. (**1985**). "Air column, reed, and player's windway interaction in musical instruments," in *Vocal Fold Physiology, Biomechanics, Acoustics and Phonatory Control*, edited by I. R. Titze and R. C. Scherer (Denver Center for the Performing Arts, Denver, CO), Chap. 35, pp. 425–452.

Bouhuys, A. (**1965**). "Sound-power production in wind instruments," J. Acoust. Soc. Am. **37**(3), 453–456.

Bouhuys, A. (**1968**). "Pressure-flow events during wind instrument playing," Ann. N. Y. Acad. Sci. **155**(1), 264–275.

Boutin, H., Fletcher, N. H., Smith, J., and Wolfe, J. (**2013**). "Lip motion, the playing frequency of the trombone and upstream and downstream impedances," in *Proceedings of the Stockholm Music Acoustics Conference (SMAC 2013)*, Stockholm, Sweden, pp. 483–489.

Boutin, H., Fletcher, N., Smith, J., and Wolfe, J. (**2014**). "Lipping down on the trombone: Phases of lip motion and pressures," in *Proceedings of the International Symposium on Musical Acoustics (ISMA 2014)*, Le Mans, France, pp. 119–124.

Bromage, S., Campbell, D. M., and Gilbert, J. (**2010**). "Open areas of vibrating lips in trombone playing," Acta Acust. Acust. **96**(4), 603–613.

Campbell, D. M. (**1999**). "Nonlinear dynamics of musical reed and brass wind instruments," Contemp. Phys. **40**, 415–431.

Caussé, R., Kergomard, J., and Lurton, X. (**1984**). "Input impedance of brass musical instruments—Comparison between experiment and numerical models," J. Acoust. Soc. Am. **75**(1), 241–254.

Chen, F.-C., and Weinreich, G. (**1996**). "Nature of the lip reed," J. Acoust. Soc. Am. **99**(2), 1227–1233.

Chen, J.-M., Smith, J., and Wolfe, J. (**2012**). "Do trumpet players tune resonances of the vocal tract?," J. Acoust. Soc. Am. **131**(1), 722–727.

Copley, D. C., and Strong, W. J. (**1996**). "A stroboscopic study of lip vibrations in trombone," J. Acoust. Soc. Am. **99**(2), 1219–1226.

Cullen, J. S., Gilbert, J., and Campbell, D. M. (**2000**). "Brass instruments: Linear stability analysis and experiments with an artificial mouth," Acta Acust. Acust. **86**(4), 704–724.

Dickens, P., Smith, J., and Wolfe, J. (**2007**). "Improved precision in acoustic impedance measurements by using calibration loads without resonances," J. Acoust. Soc. Am. **121**(3), 1471–1481.

Elliott, S. J., and Bowsher, J. M. (**1982**). "Regeneration in brass wind instruments," J. Sound Vib. **83**(2), 181–217.

Elliott, S. J., Bowsher, J. M., and Watkinson, P. (**1982**). "Input and transfer response of brass wind instruments," J. Acoust. Soc. Am. **72**(6), 1747–1760.

Eveno, P., Petiot, J.-F., Gilbert, J., Kieffer, B., and Caussé, R. (**2014**). "The relationship between bore resonance frequencies and playing frequencies in trumpets," Acta Acust. Acust. **100**(2), 362–374.

Fletcher, N. H. (**1993**). "Autonomous vibration of simple pressure-controlled valves in gas flows," J. Acoust. Soc. Am. **93**(4), 2172–2180.

Fletcher, N. H., and Tarnopolsky, A. (**1999**). "Blowing pressure, power, and spectrum in trumpet playing," J. Acoust. Soc. Am. **105**(2), 874–881.

Fréour, V., Caussé, R., and Cossette, I. (**2010**). "Simultaneous measurements of pressure, flow and sound during trumpet playing," in *Proceedings of the 10ème Congrès Français d' Acoustique (CFA 2010)*, Lyon, France.

Fréour, V., and Scavone, G. P. (**2011**). "Development of an electrolabiograph embedded in a trombone mouthpiece for the study of lip oscillation mechanisms in brass instrument performance," Can. Acoust. **39**(3), 130–131.

Fréour, V., and Scavone, G. P. (**2013**). "Acoustical interaction between vibrating lips, downstream air column, and upstream airways in trombone performance," J. Acoust. Soc. Am. **134**(5), 3887–3898.

Gilbert, J., Ponthus, S., and Petiot, J.-F. (**1998**). "Artificial buzzing lips and brass instruments: Experimental results," J. Acoust. Soc. Am. **104**(3), 1627–1632.

Hanna, N., Smith, J., and Wolfe, J. (**2012**). "Low frequency response of the vocal tract: Acoustic and mechanical resonances and their losses," in *Proceedings of Acoustics 2012*, Fremantle, Australia.

Helmholtz, H. L. F. (**1877**). *On the Sensations of Tone*, 4th ed., translated by A. J. Ellis (Dover, New York, 1954), p. 97.

Hézard, T., Fréour, V., Caussé, R., Hélie, T., and Scavone, G. (**2014**). "Synchronous multimodal measurements on lips and glottis: Comparison between two human-valve oscillating systems," Acta Acust. Acust. **100**(6), 1172–1185.

Hirschberg, A. (**1995**). "Aero-acoustics of wind instruments," in *Mechanics of Musical Instruments*, edited by A. Hirschberg, J. Kergomard, and G. Weinreich, International Centre for Mechanical Sciences, Udine, Italy (Springer-Verlag, New York), pp. 291–369.

Ishizaka, K., and Flanagan, J. L. (**1972**). "Synthesis of voiced sounds from a two-mass model of the vocal cords," Bell Syst. Tech. J. **51**, 1233–1268.

Lous, N. J. C., Hofmans, G. C. J., Veldhuis, R. N. J., and Hirschberg, A. (**1998**). "A symmetrical two-mass vocal-fold model coupled to vocal tract and trachea, with application to prosthesis design," Acta Acust. Acust. **84**, 1135–1150.

Lulich, S. M., Alwan, A., Arsikere, H., Morton, J. R., and Sommers, M. S. (**2011**). "Resonances and wave propagation velocity in the subglottal airways," J. Acoust. Soc. Am. **130**(4), 2108–2115.

Martin, D. W. (**1942**). "Lip vibrations in a cornet mouthpiece," J. Acoust. Soc. Am. **13**, 305–308.

Mukai, M. S. (**1992**). "Laryngeal movement while playing wind instruments," in *Proceedings of the International Symposium Musical Acoustics (ISMA 92)*, Tokyo, Japan, pp. 239–242.

Newton, M. J., Campbell, D. M., and Gilbert, J. (**2008**). "Mechanical response measurements of real and artificial brass players lips," J. Acoust. Soc. Am. **123**(1), EL14–EL20.

Pelorson, X., Hirschberg, A., van Hassel, R. R., and Wijnands, A. P. J. (**1994**). "Theoretical and experimental study of quasisteady flow separation within the glottis during phonation," J. Acoust. Soc. Am. **96**(6), 3416–3431.

Savitzky, A., and Golay, M. J. E. (**1964**). "Smoothing and differentiation of data by simplified least squares procedures," Anal. Chem. **36**(8), 1627–1639.

Smith, J. R. (**1995**). "Phasing of harmonic components to optimize measured signal-to-noise ratios of transfer functions," Meas. Sci. Technol. **6**, 1343–1348.

Smith, J. R., Henrich, N., and Wolfe, J. (**1997**). "The acoustic impedance of the Bœhm flute: Standard and some non-standard fingerings," Proc. Inst. Acoust. **19**, 315–320.

Strong, W. J., Dudley, J. D. (**1993**). "Simulation of a player-trumpet system," in *Proceedings of the Stockholm Music Acoustics Conference (SMAC 93)*, Stockholm, Sweden, pp. 520–524.

Tarnopolsky, A., Fletcher, N., Hollenberg, L., Lange, B., Smith, J., and Wolfe, J. (**2005**). "The vocal tract and the sound of a didgeridoo," Nature **436**(7), 39.

Tarnopolsky, A. Z., Fletcher, N. H., Hollenberg, L. C. L., Lange, B. D., Smith, J., and Wolfe, J. (**2006**). "Vocal tract resonances and the sound of the Australian didjeridu (yidaki): I. Experiment," J. Acoust. Soc. Am. **119**, 1194–1204.

Wolfe, J., and Smith, J. (**2008**). "Acoustical coupling between lip valves and vocal folds," Acoust. Aust. **36**(1), 23–27.

Yoshikawa, S. (**1995**). "Acoustical behavior of brass player's lips," J. Acoust. Soc. Am. **97**(3), 1929–1939.

Yoshikawa, S., and Muto, Y. (**2003**). "Lip-wave generation in horn players and the estimation of lip-tissue elasticity," Acta Acust. Acust. **89**, 145–162.